Non-equilibrium lattice fluid modeling of gas solubility in HAB-6FDA polyimide and its thermally rearranged analogs

Michele Galizia[a], Kevin A. Stevens[a], Zachary P. Smith[b],

Donald R. Paul[a] and Benny D. Freeman[a]*

[a] *John J. McKetta Jr. Department of Chemical Engineering, The University of Texas at Austin, 200 E. Dean Keeton Street, 78712 Austin, Center for Energy and Environmental Resources, 10100 Burnet Rd., Building 133 (CEER), 78758 Austin, TX, USA*
[b] *Department of Chemical Engineering, Massachusetts Institute of Technology 25 Ames Street, 02142 Cambridge, MA, USA*

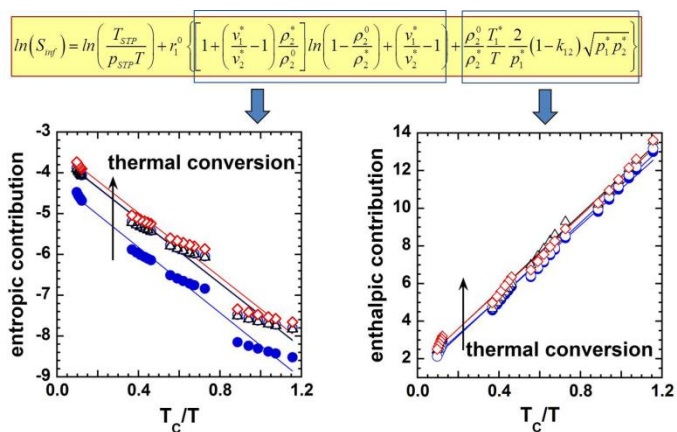## REVISED MANUSCRIPT

*Corresponding author (Benny D. Freeman)
freeman@che.utexas.edu
(512) 232 2803

For Table of Contents use only

Non-equilibrium lattice fluid modeling of gas solubility in HAB-6FDA polyimide and its thermally rearranged analogs

M. Galizia, K.A. Stevens, Z.P. Smith, D.R. Paul, B.D Freeman

$$ln\left(S_{inf}\right) = ln\left(\frac{T_{STP}}{p_{STP}T}\right) + r_1^0\left\{\left[1+\left(\frac{v_1^*}{v_2^*}-1\right)\frac{\rho_2^*}{\rho_2^0}\right]ln\left(1-\frac{\rho_2^0}{\rho_2^*}\right)+\left(\frac{v_1^*}{v_2^*}-1\right)+\frac{\rho_2^0}{\rho_2^*}\frac{T_1^*}{T}\frac{2}{p_1^*}\left(1-k_{12}\right)\sqrt{p_1^*p_2^*}\right\}$$

Abstract

For the first time, a theoretical analysis of gas sorption, based on the non-equilibrium lattice fluid (NELF) model, in chemically-imidized HAB-6FDA polyimide and its thermally rearranged analogs is presented. Due to the inaccessibility of pVT data in the rubbery region, the characteristic lattice fluid parameters of the polymers considered in this study were obtained from a collection of infinite dilution solubility data at multiple temperatures. Hydrogen, nitrogen and methane sorption isotherms at 35°C were fit to the NELF model using one adjustable parameter, i.e., the polymer-penetrant binary interaction parameter, k_{12} . The optimal value of k_{12} for each polymer-penetrant pair was used to predict hydrogen, nitrogen and methane sorption isotherms at other temperatures and at pressures up to 6 MPa. For carbon dioxide, a second adjustable parameter, the swelling coefficient, was introduced to account for sorption-induced matrix dilation. The ideal solubility-selectivity is also predicted for several gas pairs. The increase in gas sorption in thermally rearranged samples relative to their polyimide precursor is essentially due to entropic effects, i.e., to the increase in non-equilibrium fractional free volume during thermal rearrangement.

1. Introduction

Due to their unusual combinations of high gas permeability and selectivity, thermally rearranged (TR) polymers have attracted interest for membrane gas separation[1]. These materials, first reported by Park et al.[2], exhibit transport properties that, in some cases, surpass the upper bound defined by Robeson in 2008[3,4,5]. TR polymers are formed by chemically reacting solvent-soluble polyimides, via thermal treatment in the solid state, to insoluble, perhaps crosslinked polybenzoxazoles (PBOs)[2,6,7,8]. Since PBOs are insoluble in common organic solvents, it is not possible to exploit classic solution-casting procedures to obtain thin membranes. On the other hand, the lack of solubility in organic solvents allows these polymers to be used in chemically challenging environments. The latter aspect is important for natural gas sweetening, where the presence of impurities, such as higher hydrocarbons and aromatics, can adversely affect separation efficiency and membrane integrity[9].

The transport properties exhibited by TR polymers are ascribed to a favorable size and distribution of free volume elements[1,6,7,8]. For example, the increase in gas solubility with increasing extent of thermal conversion has been attributed to increases in excess fractional free volume[6]. Such results are further supported by separate PALS analysis and simulations based on Monte Carlo methods[10]. These studies indicated an increase in the average size of free volume cavities with increasing extent of thermal conversion[10]. However, in a recent study, Robeson et al.[11] reported that the unique performance exhibited by TR polymers and other glassy materials, such as PIMs, relies on the unusual combination of high diffusivity, high

1

diffusivity selectivity and high gas solubility. This important finding further motivates the fundamental analysis of gas sorption in TR polymers presented in this study.

Previous gas transport studies of TR polymers were essentially experimental[6,7], so this study represents the first theoretical analysis of gas sorption in HAB-6FDA and its TR analogs based on a rigorous thermodynamic approach. A crucial point in this analysis is the estimation of polymer's lattice fluid characteristic parameters. Since these polymers have extremely high glass transition temperatures[6], their thermodynamic properties in the rubbery region, which are usually exploited to estimate the lattice fluid parameters of polymers, are not experimentally accessible. To circumvent this challenge, the lattice fluid parameters of HAB-6FDA and its TR analogs were determined using the approach first reported by Galizia et al.[12], which requires only sorption data in the limit of infinite dilution.

The analysis presented in this study rationalizes previous experimental findings. In particular, the separate analysis of entropic and enthalpic contributions to gas solubility improves fundamental understanding of gas sorption behavior of TR polymers. To the best of our knowledge, no other model permits such a detailed fundamental analysis of gas sorption in glassy polymers.

2. Theoretical background

The non-equilibrium lattice fluid (NELF) model extends the Sanchez-Lacombe equation of state[13] to the non-equilibrium state of glassy polymers[14]. Compared to other models for gas sorption in glassy polymers[15,16], the NELF model exhibits remarkable predictive

2

power[12,14,17,18,19,20]. This model requires, for the penetrant and the polymer, the same characteristic parameters as the corresponding equilibrium model, and it uses the same mixing rules to estimate properties of polymer-penetrant mixture[14]. The polymer and penetrant characteristic lattice fluid parameters (i.e., T^*, p^* and ρ^*) can be obtained from the literature or directly estimated using thermodynamic data for the pure components[14]. Typically, the three scaling parameters for the polymer are obtained by fitting experimental pVT data in the rubbery region to the Sanchez-Lacombe equation of state[13]. The characteristic temperature of component *i*, T_i^*, quantifies the interaction energy between two molecular segments occupying adjacent positions on the lattice[12]. The characteristic pressure, p_i^*, provides an estimate of the cohesive energy density of the species *i* at close-packed conditions (i.e., at 0 K) [12]. Finally, ρ_i^* is the density of the component *i* at close-packed conditions[12]. In this study, we label the penetrant with subscript "1" and the polymer with subscript "2".

According to the approach proposed by Sarti et al.[14], the thermodynamic state of a mixture containing a low molecular weight penetrant and a glassy polymer can be described by the classical variables, i.e. temperature, pressure and composition, plus the polymer density, which explicitly accounts for the non-equilibrium state of glassy polymers. The NELF model provides an expression for the non-equilibrium chemical potential of the penetrant, which can be used to calculate gas and vapor solubility in glassy polymers. For such calculations, the following set of equations are solved: *i)* the phase equilibrium condition, which can be expressed by equating the non-equilibrium chemical potential of the penetrant in the glassy polymer with the equilibrium penetrant chemical potential in the contiguous, external fluid phase, and *ii)* the

Sanchez-Lacombe equation of state for the pure penetrant in the external fluid phase[12,14]. The relevant NELF model variables and equations are summarized in Table 1.

During sorption of non-swelling penetrants, such as light gases (e.g., He, H_2, O_2, N_2 and CH_4), the polymer density does not change noticeably. Thus, the solubility of such non-swelling penetrants can be predicted with just one fitting parameter, i.e., the polymer-penetrant interaction parameter, k_{12}, which measures the departure of polymer-penetrant binary interaction from the geometric mixing rule, as predicted by Hildebrand's theory[21]. Since k_{12} does not show any dependence on temperature or composition[13], it can be estimated for each polymer-penetrant pair by fitting sorption data at one reference temperature. Then, sorption isotherms can be predicted at any other temperature with no additional adjustable parameters[17].

When considering strongly sorbing penetrants, such as CO_2 at high pressure or condensable vapors, changes in polymer density (i.e., swelling) due to sorption must be considered[12,18,22]. Experimental dilation data can be used to determine the actual value of polymer density at any temperature and penetrant partial pressure[22]. Alternatively, if experimental dilation data are not available, the polymer density at each penetrant partial pressure can be obtained indirectly from sorption data. Indeed, based on a review of experimental dilation data available in the literature, Sarti et al.[23] assumed a linear correlation between the polymer density and the penetrant partial pressure, i.e.:

$$\rho_2(p) = \rho_2^0 \left(1 - k_{sw} p\right) \qquad \text{(Eq. 1)}$$

where ρ_2^0 is the density of the pure polymer, which is measured experimentally, k_{sw} is the swelling coefficient, and p is the penetrant partial pressure. So, in the absence of experimental

4

dilation data, k_{sw} is treated as a fitting parameter whose value is adjusted using a single experimental sorption datum at high pressure, where significant polymer dilation is expected to take place[12,22,23]. Then, using Eq. 1, it is possible to estimate, at fixed temperature and penetrant partial pressure, polymer density. As reported elsewhere[12,22,23], the polymer density estimated using this simple approach agrees reasonably well with experimental data. Thus, for swelling penetrants, sorption isotherms can be described by two fitting parameters, i.e. k_{12} and k_{sw} at one reference temperature, while just one adjustable parameter, k_{sw}, is required at any other temperature. So, compared to other models for gas sorption in glassy polymers[15,16], the NELF model has better predictive capability.

The phase equilibrium condition significantly simplifies in the limit of vanishing pressure. In this case, the infinite dilution sorption coefficient, S_{inf}, from the NELF model is[12,23]:

$$ln\left(S_{inf}\right)=ln\left(\frac{T_{STP}}{p_{STP}T}\right)+r_1^0\left\{\left[1+\left(\frac{v_1^*}{v_2^*}-1\right)\frac{\rho_2^*}{\rho_2^0}\right]ln\left(1-\frac{\rho_2^0}{\rho_2^*}\right)+\left(\frac{v_1^*}{v_2^*}-1\right)+\frac{\rho_2^0}{\rho_2^*}\frac{T_1^*}{T}\frac{2}{p_1^*}\left(1-k_{12}\right)\sqrt{p_1^*p_2^*}\right\}$$

(Eq. 2)

where the subscript STP indicates the standard temperature and pressure conditions (i.e., 273 K and 1 atm). The meaning of variables in Eq. 2 is reported in Table 1.

Table 1. List of parameters and equations for the NELF model. Subscript i stands for penetrant (1) and polymer (2) species, respectively.

symbol	property	definition
M_i	Molar mass of species i	
T_i^*	Characteristic temperature of pure component i	
p_i^*	Characteristic pressure of pure component i	
ρ_i^*	Characteristic density of pure component i	
k_{ij}	Binary parameter	
ρ_i	Density of species i	
ρ	Density of the mixture	
ω_i	Mass fraction of species i	
Φ_i	Volume fraction of species i at close packed conditions	$\Phi_i = \dfrac{\omega_i/\rho_i^*}{\sum_i \omega_i/\rho_i^*}$
r_i^0	Number of lattice cells occupied by a molecule of pure component i	
r_i	Number of lattice cells occupied by a molecule in mixture	
$\tilde{T}_i$	Reduced temperature of pure component i	$\tilde{T}_i = \dfrac{T}{T_i^*}$
$\tilde{p}_i$	Reduced pressure of pure component i	$\tilde{p}_i = \dfrac{p}{p_i^*}$
$\tilde{\rho}_i$	Reduced density of pure component i	$\tilde{\rho}_i = \dfrac{\rho_i}{\rho_i^*}$
$\tilde{T}$	Reduced temperature of the mixture	$\tilde{T} = \dfrac{T}{T^*}$
$\tilde{p}$	Reduced pressure of the mixture	$\tilde{p} = \dfrac{p}{p^*}$
$\tilde{\rho}$	Reduced density of the mixture	$\tilde{\rho} = \dfrac{\rho}{\rho^*}$
v_i^*	Volume occupied by a mole of lattice site of pure component i	$v_i^* = \dfrac{RT_i^*}{p_i^*}$
Mixing rules		

T^*	Characteristic temperature (binary mixtures)	$T^* = \dfrac{p^*}{\dfrac{\Phi_1 p_1^*}{T_1^*} + \dfrac{\Phi_2 p_2^*}{T_2^*}}$ (Eq.3)
p^*	Characteristic pressure (binary mixtures)	$p^* = \Phi_1 p_1^* + \Phi_2 p_2^* - \Phi_1 \Phi_2 \left[p_1^* + p_2^* - 2(1-k_2)\sqrt{p_1^* p_2^*} \right]$ (Eq.4)
ρ^*	Characteristic density (binary mixtures)	$\dfrac{1}{\rho^*} = \dfrac{\omega_1}{\rho_1^*} + \dfrac{\omega_2}{\rho_2^*}$ (Eq.5)
Sanchez-Lacombe EoS and expression of equilibrium and non-equilibrium chemical potential		
SL-EOS for pure penetrant		$\tilde{\rho}_1 = 1 - \exp\left[-\dfrac{\tilde{\rho}_1^2}{\tilde{T}_1} - \dfrac{\tilde{p}_1}{\tilde{T}_1} - \tilde{\rho}_1\left(1 - \dfrac{1}{r_1^0}\right) \right]$ (Eq.6)
SL-EOS for the binary mixture		$\tilde{\rho} = 1 - \exp\left[-\dfrac{\tilde{\rho}^2}{\tilde{T}} - \dfrac{\tilde{p}}{\tilde{T}} - \tilde{\rho}\left(1 - \dfrac{\Phi_1}{r_1}\right) \right]$ (Eq.7)
Equilibrium chemical potential of pure penetrant		$\dfrac{\mu_1^0}{RT} = r_1^0\left[-\dfrac{\tilde{\rho}_1}{\tilde{T}_1} + \dfrac{\tilde{p}_1}{\tilde{T}_1 \tilde{\rho}_1} + \dfrac{1}{r_1^0}\ln\tilde{\rho}_1 + \dfrac{1-\tilde{\rho}_1}{\tilde{\rho}_1}\ln\left(1-\tilde{\rho}_1\right) \right]$ (Eq.8)
Equilibrium chemical potential of penetrant in mixture		$\dfrac{\mu_1}{RT} = 1 - \Phi_1 + \ln\Phi_1 + \dfrac{\tilde{\rho} M_1 \Delta p^*}{RT \rho_1^*}(1-\Phi_1)^2 + r_1^0\left[-\dfrac{\tilde{\rho}}{\tilde{T}_1} + \dfrac{\tilde{p}_1}{\tilde{T}_1 \tilde{\rho}} + \dfrac{1}{r_1}\ln\tilde{\rho} + \dfrac{1-\tilde{\rho}}{\tilde{\rho}}\ln\left(1-\tilde{\rho}\right) \right]$ (Eq.9)
Chemical potential of species i in the non-equilibrium state		$\dfrac{\mu_i^{ne}}{RT} = \ln\left(\tilde{\rho}\phi_i\right) - \left(r_i^0 + \dfrac{r_i - r_i^0}{\tilde{\rho}}\right)\ln\left(1-\tilde{\rho}\right) - r_i - \tilde{\rho}\dfrac{r_i^0 v_i^*}{RT}\left[p_i^* + \sum_{j=1}^{N_p+1} \phi_j\left(p_j^* - \Delta p_{ij}^*\right) \right]$ (Eq.10)

Eq. 2 can be used to estimate the polymer characteristic lattice fluid parameters when infinite dilution solubility data are experimentally available for a series of penetrants[12]. This approach can be of great utility for ultra-high T_g polymers, whose thermodynamic data in the rubbery region often are not experimentally accessible. This method has been successfully used to estimate lattice fluid parameters for high T_g glassy polymers such as poly(trimethylsilyl norbornene)[12] and Matrimid® polyimide[24]. The lattice fluid parameters for HAB-6FDA

polyimide and its TR analogs have been determined by fitting Eq. 2 to experimental infinite dilution solubility data available at multiple temperatures for hydrogen, helium, nitrogen, methane and carbon dioxide[25,26,27]. In Eq. 2, the polymer-penetrant interaction parameter, k_{12}, explicitly appears. For light gases in the limit of vanishing pressure, a reasonable representation of infinite dilution sorption data can be obtained assuming $k_{12} = 0$[12,21].

The solubility coefficient in Eq. 2 contains an entropic contribution (ϕ_S) and an enthalpic contribution (ϕ_H)[12,28]. ϕ_S and ϕ_H represent the entropic and the energetic contributions to the penetrant chemical potential in the glassy mixture, respectively[12]. Thus, Eq. 2 can be re-written as follows:

$$ln\left(S_{inf}\right) = ln\left(\frac{T_{STP}}{p_{STP}T}\right) + \phi_S + \phi_H \qquad \text{(Eq. 11)}$$

where

$$\phi_S = r_1^0\left\{\left[1 + \left(\frac{v_1^*}{v_2^*} - 1\right)\frac{\rho_2^*}{\rho_2^0}\right]ln\left(1 - \frac{\rho_2^0}{\rho_2^*}\right) + \left(\frac{v_1^*}{v_2^*} - 1\right)\right\} \qquad \text{(Eq. 12)}$$

and

$$\phi_H = r_1^0\left\{\frac{\rho_2^0}{\rho_2^*}\frac{T_1^*}{T}\frac{2}{p_1^*}\left(1 - k_{12}\right)\sqrt{p_1^* p_2^*}\right\} \qquad \text{(Eq. 13)}$$

In this study, we report both the entropic and the enthalpic contributions of the infinite dilution solubility coefficient, to shed fundamental light on the molecular origin of the sorption behavior of TR polymers.

3. Experimental

The relevant properties of the polymers considered in this study are summarized in Table 2. Details about the synthesis and the casting procedure are reported elsewhere[6] and are also briefly recalled in the Supporting Information. In the following, the TR samples are labelled TRX-Y, where X and Y are the temperature and the duration of thermal treatment, respectively. Details of gas sorption measurements are reported elsewhere[25,26,27].

Table 2. *Relevant chemical and physical properties of the polymers considered in this study.*

	density[†] (Kg/L)	*T_g[‡] (°C)*	*conversion[‖] (%)*
HAB-6FDA	*1.407 ± 0.009*	255	0
TR350-1h	*1.398 ± 0.009*	> 450	39
TR400-1h	*1.400 ± 0.009*	> 450	60
TR450-30 min	*1.340 ± 0.01*	> 450	76

[†] measured at room temperature with an Archimedes' balance[6].
[‡] from Differential Scanning Calorimetry measurements[6].
[‖] Conversion of the polyimide precursor to the final TR polymer is defined as: 100×(actual mass loss)/(theoretical mass loss). The actual mass loss was measured via thermogravimetric analysis. The theoretical mass loss is the mass loss expected in the case of complete thermal conversion[6].

4. Results and discussion

4.1 Estimation of Lattice Fluid parameters for HAB-6FDA and TR-samples. Due to the inaccessibility of pVT data in the rubbery state, the characteristic lattice fluid parameters for the HAB-6FDA polyimide precursor and its TR analogs were estimated using the method reported by Galizia et al.[12]. That is, Eq. 2 was used to simultaneously fit, for each polymer, experimental infinite dilution solubility coefficients for different light gases, i.e. H_2, He, N_2, CH_4 and CO_2, at multiple temperatures, ranging from -10 to 50°C[25,26,27]. In this procedure, the polymer characteristic lattice

fluid parameters, T^*, p^* and ρ^*, were treated as fitting parameters and adjusted to the experimental sorption data, while the polymer-penetrant interaction parameter, k_{12}, was set equal to zero[12]. Since sorption data for polar or halogenated penetrants are not included in the fitting procedure, assuming $k_{12} = 0$ is a reasonable approximation[12,28].

The polymer density, which explicitly appears in Eq.2, was estimated at different temperatures using a reasonable value of the thermal expansion coefficient, α_v, and the experimental density measured at room temperature (cf., Table 2). The thermal expansion coefficients for HAB-6FDA and its TR samples are not available in the literature, but the values for other fluorinated polyimides, such as 6FDA-ODA and 6FDA-6FpDA, are reported[29] or can be calculated from experimental pVT data[29]. The two fluorinated polyimides mentioned above, 6FDA-ODA and 6FDA-6FpDA have similar thermal expansion coefficients, i.e., $2 \times 10^{-4} K^{-1}$ [29]. Moreover their chemical structures are similar to that of HAB-6FDA. Thus, absent specific data for HAB-6FDA and its TR samples, the density values of the polymers were estimated at different temperatures by assuming $\alpha_v = 2 \times 10^{-4} K^{-1}$. Thermal expansion coefficients reported in the literature for other polyimides, such as Matrimid® polyimide[30] and Ultem® 1000 poly(ether-imide)[31] (i.e., $9 \times 10^{-5} K^{-1}$) do not depart markedly from the value assumed in this study. For example, if α_v is allowed to change between $9 \times 10^{-5} K^{-1}$ and $2 \times 10^{-4} K^{-1}$, the change in polymer density for HAB-6FDA and its TR analogs is less than 0.4% over the temperature range considered. Moreover, the density of glassy polymers is expected to change little with temperature over the range of temperature considered here[17]. For instance, for the polymers considered in this study, the density change does not exceed 1% over the range of temperatures explored (-10 to 50°C). If α_v

is allowed to change between $9 \times 10^{-5} K^{-1}$ and $2 \times 10^{-4} K^{-1}$, the effect on calculated gas solubility is less than 3%. Thus, assuming $\alpha_v = 2 \times 10^{-4} K^{-1}$ for HAB-6FDA and its TR analogs is physically reasonable and has little bearing on the results from this study.

In Fig. 1, the infinite dilution sorption coefficients estimated from experimental data at higher pressures for different gases at multiple temperatures[6,25,26,27] are reported in a parity plot, along with the respective theoretical values estimated from Eq. 2, using T_2^*, p_2^* and ρ_2^* as fitting parameters. The data and model are in reasonable agreement for all penetrant-polymer pairs over the range of temperatures considered. In the case of light, less soluble gases (H_2 and N_2), the maximum deviation of calculated infinite dilution sorption data from the experimental values is ±30%. In the case of more soluble gases, such as CH_4 and CO_2, the maximum deviation is ±10%. These deviations are comparable to those reported in the literature[12,24] for other polymer-penetrant systems, where deviations ranging from 20 to 58% were observed.

The uncertainties in the lattice fluid parameters of HAB-6FDA and its TR analogs were estimated using a likelihood-based statistical analysis of data[32] and are less than 5%. For comparison purposes, in Table 3 we also report the characteristic lattice fluid parameters for other fluorinated polyimides, i.e., 6FDA-ODA and 6FDA-6FpDA[29].

To test the reliability of the lattice fluid parameters determined using Eq. 2 with k_{12} = 0, a sensitivity analysis was performed. In particular, the effect of a perturbation of k_{12} on the polymer's lattice fluid parameters was quantified. Eq. 2 was used to fit the experimental infinite dilution sorption data assuming, for each penetrant, the values of k_{12} reported in Table 4, which were obtained from the NELF modeling of sorption data in a wide pressure range (c.f., § 4.2 and

11

4.3). The corresponding change of T_2^*, p_2^* and ρ_2^* relative to the values reported in Table 3 is within their uncertainty, which is also reported in Table 3. Similar results were obtained for TR samples. So, one can conclude that the SL parameters calculated from Eq.2 assuming $k_{12} = 0$ are reasonable. The same sensitivity analysis was used by Galizia et al.[12] to analyze the lattice fluid parameters determined for a novel poly(acetylene), PTMSN.

The results of this sensitivity analysis agree with previous literature reports[12,28], which suggest that, in the limit of infinite dilution, the approximation of $k_{12} = 0$ is reasonable unless polar or halogenated penetrant are considered. Indeed, sorption of polar (e.g., acetone, methanol, ethanol) and fluorinated (e.g., fluoromethane, fluoroethane) penetrants in polymers shows large deviations from the Hildebrand rule[12,26,28]. Interestingly, the resulting lattice fluid parameters for HAB-6FDA (cf., Table 3) compare reasonably well to those reported for other partially fluorinated polyimides, such as 6FDA-ODA and 6FDA-6FpDA[29].
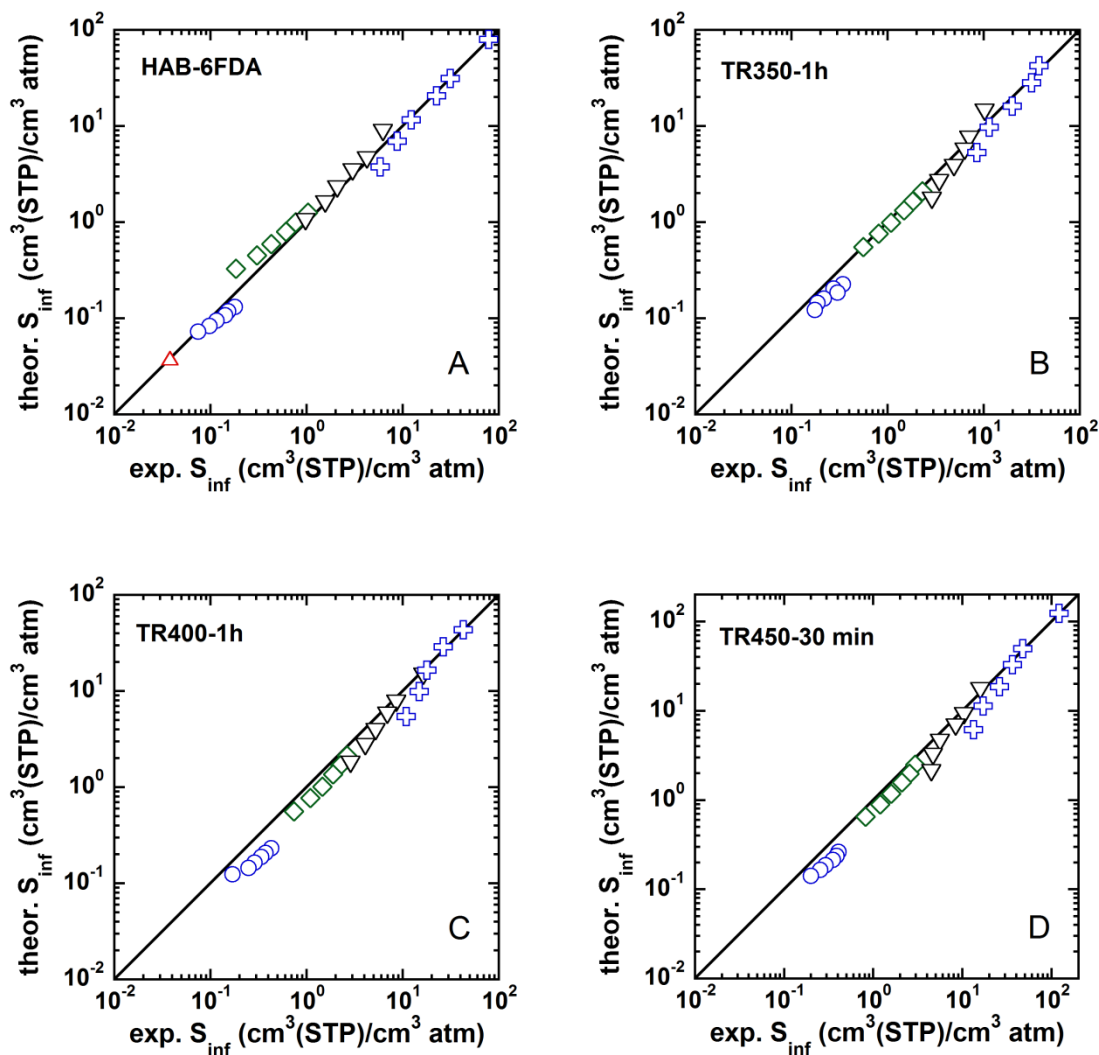
Figure 1. *Theoretical vs. experimental infinite dilution solubility coefficients for different gases at multiple temperatures (-10 to 50 °C). A): HAB-6FDA; B) TR350-1h; C) TR400-1h; D) TR450-30 min. Red triangle: helium; blue circles: hydrogen; green diamonds: nitrogen; black triangles: methane; blue crosses: carbon dioxide. The solid line represents the parity line.*

As shown in Table 3, the lattice fluid parameters of TR samples reflect the more rigid structure of these polymers and the different size and distribution of free volume elements compared to the HAB-6FDA polyimide. For example, the value of T^* increases with increasing degree of thermal conversion. This result is not surprising, since TR samples are more rigid than the HAB-6FDA precursor, and their stiffness increases with increasing thermal conversion. Since T^*

quantifies the interaction energy between adjacent polymer chains, it provides indirect information regarding polymer stiffness. Conversely, p^* slightly decreases with increasing degree of thermal conversion. This trend reflects the lower cohesive energy densities of TR samples relative to HAB-6FDA polyimide. Similarly, ρ^* decreases slightly with increasing thermal conversion, which is consistent with the slight decrease in density observed for TR polymers relative to HAB-6FDA polyimide and with the higher non-equilibrium free volume shown by TR polymers relative to the polyimide precursor[6].

Table 3. *Lattice fluid parameters for polymers and penetrants considered in this study. The characteristic parameters of other fluorinated polyimides[29] are reported for comparison. The uncertainties in the lattice fluid parameters were calculated using a likelihood-based statistical analysis of data[32].*

polymer	T^* (K)	p^* (MPa)	ρ^* (kg/L)	source
HAB-6FDA	720.0 ± 41	481.1 ± 20	1.609 ± 0.039	this study
TR350-1h	855.2 ± 42	450.0 ± 20	1.600 ± 0.039	this study
TR400-1h	867.1 ± 7	450.0 ± 1.4	1.600 ± 0.039	this study
TR450-30 min	930.0 ± 23	446.9 ± 7.3	1.528 ± 0.037	this study
6FDA-ODA	804.3	526.6	1.700	[29]
6FDA-6FpDA	751.0	474.0	1.810	[29]
penetrant				
H_2	46	37	0.078	[28]
N_2	145	160	0.943	[28]
CH_4	215	250	0.500	[28]
CO_2	300	630	1.515	[28]

4.2 Predicting gas sorption in HAB-6FDA polyimide. To calculate hydrogen, nitrogen and methane sorption in HAB-6FDA, the polymer density was assumed, at each temperature, to be independent of penetrant partial pressure (i.e., negligible polymer swelling was assumed). Conversely, the polymer density was calculated, at each temperature, using the appropriate value of the thermal expansion coefficient[29].

Hydrogen solubility in HAB-6FDA was reported by Smith et al.[25]. As typically observed for light gas sorption in polymers, hydrogen sorption isotherms are almost linear with pressure, and solubility decreases with increasing temperature. In Fig. 2-A, the experimentally determined hydrogen solubility is reported as a function of pressure, along with NELF model calculations. The polymer-penetrant binary parameter, k_{12}, was optimized to the experimental data at 35°C and that value, -0.1, was used to estimate, in a completely predictive fashion, the solubility at all other temperatures. Good agreement was found between the model predictions and the experimental sorption isotherms over the entire range of pressures considered, at all temperatures, with an average deviation of less than 4.5%. The best fit values of k_{12} for each gas/polymer pair are recorded in Table 4. Sorption isotherms can be predicted over a broad range of pressures with $k_{sw} = 0$, as expected for non-swelling penetrants.

Table 4. *Values of penetrant-polymer binary interaction parameters and swelling coefficients at 35°C.*

	H_2	N_2	CH_4	CO_2	
	k_{12}			k_{12}	k_{sw} at 35°C (MPa^{-1})
HAB-6FDA	*-0.10*	*0.085*	*0.06*	*-0.01*	*0.010*
TR350-1h	*-0.05*	*0.025*	*0.015*	*-0.06*	*0.013*
TR400-1h	*-0.26*	*-0.02*	*-0.08*	*-0.09*	*0.013*
TR450-30 min	*-0.24*	*-0.03*	*-0.03*	*-0.09*	*0.020*

Nitrogen sorption isotherms in HAB-6FDA at multiple temperatures[27] are presented in Fig. 2-B. Due to the higher condensability of nitrogen, its solubility is greater than that of hydrogen. The binary parameter, k_{12}, was adjusted to the sorption data at 35°C and that value, 0.085, was used to predict sorption isotherms at other temperatures. The quantitative agreement between the model and the data is reasonably good up to 4 MPa. Greater deviations, by about 13%, are observed at pressures higher than 4 MPa. However, we believe this deviation can be accepted, since the model is used in a predictive fashion. The likely sources of this deviation could be the uncertainty in the experimental data, as well as the uncertainty in the polymer lattice fluid parameters.

The same procedure was used to model methane sorption isotherms in HAB-6FDA[27] (Fig. 2-C). The model outcomes agree reasonably well with the experimental data over the range of pressures and temperatures considered.

In summary, hydrogen, nitrogen and methane solubility isotherms in HAB-6FDA can be predicted at multiple temperatures and up to 6MPa with one adjustable parameter per gas (i.e., k_{12}), which does not depend on temperature, pressure or composition. Thus, once k_{12} has been

optimized to the experimental data at a reference temperature (35°C in this case), sorption isotherms at any other temperature can be predicted with no adjustable parameters. This result is remarkable, since the Dual Mode Model[15,16] would require, for each penetrant, three adjustable parameters at each temperature. Moreover, as reported by Bondar et al.[33], the three Dual Mode parameters, k_D, C_H' and b depend on the range of pressures used to fit the experimental data.
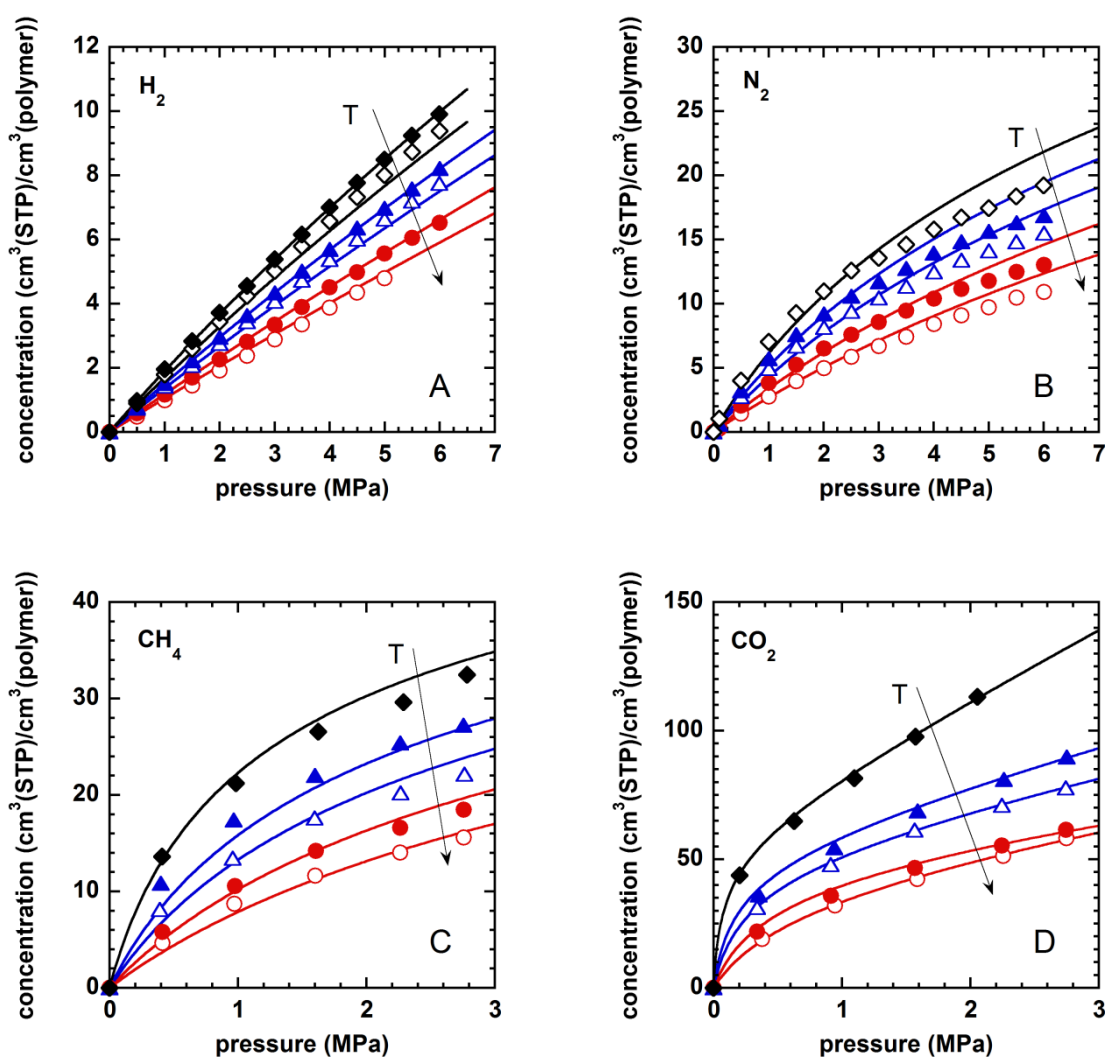

Figure 2. *Gas solubility in HAB-6FDA polyimide. A) H_2, B) N_2, C) CH_4, D) CO_2. Black filled diamonds: -10°C; black open diamonds: 0°C; blue filled triangles: 10°C; blue open triangles: 20°C; red filled circles: 35°C; red open circles: 50°C. Solid lines: NELF model calculations.*

The best fit values of k_{12} are recorded in Table 4. For hydrogen this parameter is negative (i.e., k_{12} = - 0.1). This negative deviation from the geometric mean rule indicates more favorable polymer-penetrant interactions than those predicted by the Hildebrand's theory, which assumes k_{12} = 0. Negative deviations from the geometric mean rule were also reported for hydrogen sorption in Matrimid® polyimide, polysulfone and PDMS[17]. Conversely, for nitrogen and methane, k_{12} is slightly positive (0.085 and 0.06, respectively). Compared to other gases, the greater departure of k_{12} from zero for hydrogen might also be partially due to the uncertainty in the hydrogen sorption data, which is greater than that of other more condensable gases, since hydrogen is only sparingly soluble in polymers[17,25,26].

The modeling procedure is slightly different when considering carbon dioxide. Since carbon dioxide sorbs into the polymer to a much greater extent than the other penetrants[27], it produces a non-negligible matrix swelling[34]. Therefore, an additional adjustable parameter, the swelling coefficient, k_{sw}, is required. As discussed in the theoretical section, the polymer density is assumed to linearly decrease with increasing penetrant partial pressure (Eq. 1), so only one parameter, k_{sw}, is used to account for polymer dilation effects. To model carbon dioxide sorption in HAB-6FDA polyimide, the following two-step procedure was used: *i)* the polymer-penetrant binary parameter, k_{12}, was adjusted to the experimental sorption isotherm at 35°C in the low-pressure region, where matrix swelling is negligible, and this value of k_{12} was used to calculate the sorption isotherms at all other temperatures, and *ii)* the swelling coefficient, k_{sw}, was adjusted, at each temperature, to the experimental sorption data at high pressure, where polymer dilation becomes significant. Thus, carbon dioxide sorption at 35°C was calculated

using two adjustable parameters, i.e., k_{12} and k_{sw}, while, at other temperatures, only one adjustable parameter, k_{sw}, is required. Indeed, sorption changes with temperature, and the extent of polymer dilation depends, in turn, on the amount of penetrant sorbed in the polymer. Therefore, to predict CO_2 sorption at temperatures other than 35°C, just one sorption datum in the high pressure region is needed. As reported in Fig. 2-D, the calculated CO_2 solubility shows reasonable agreement with the experimental data. The optimal value of k_{12} (i.e., - 0.01) is very close to zero, so penetrant-polymer interactions deviate only slightly from the geometric mean rule. So, also for CO_2 the NELF model shows a greater predictive ability compared to other models, which would require more adjustable parameters.

As shown in Fig. 3, the swelling coefficient decreases with increasing temperature. Since carbon dioxide sorption decreases with increasing temperature, less matrix dilation is required, at a given pressure, to accommodate CO_2 molecules at higher temperatures. When considering carbon dioxide sorption in HAB-6FDA at 35°C, the best fit value of k_{sw} is 0.01 MPa^{-1}, which is close to the values reported in the literature for carbon dioxide sorption in other high–performance thermoplastics, such as Teflon® AF and Matrimid® polyimide [18,23]. The possibility of predicting the CO_2 sorption induced polymer swelling with no additional adjustable parameters provides a significant gain in fundamental understanding of gas sorption in TR polymers. To the best of our knowledge, no information about the dimensional stability of these materials in the presence of CO_2 has been reported so far.
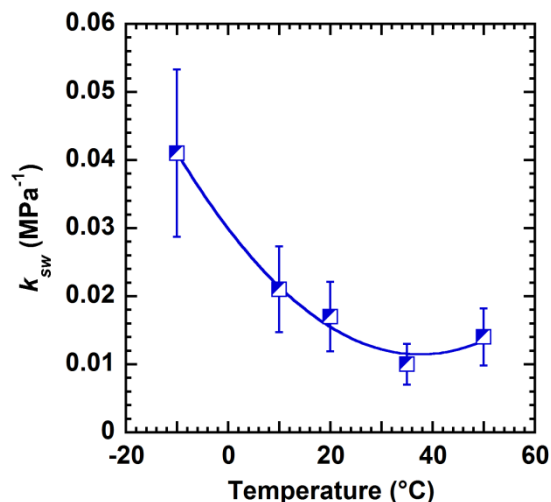
Figure 3. *Swelling coefficient for CO_2 sorption in HAB-6FDA at multiple temperatures. The curve serves to guide the eye.*

4.3 Predicting gas sorption in thermally rearranged samples. The modeling procedure described in the previous section was used to calculate hydrogen, nitrogen, methane and carbon dioxide sorption in TR samples at multiple temperatures. Three TR samples were considered, which were obtained by treating the polyimide precursor at different temperatures for a prescribed time[6,7,27]. The extent of thermal rearrangement increases in the following order: TR350-1h < TR400-1h < TR450-30min (cf., Table 2). As reported by Smith et al.[6], gas sorption in thermally rearranged samples is greater than that in the HAB-6FDA polyimide precursor, and it increases with increasing degree of thermal conversion. The observed increase in gas solubility was ascribed to an increase of excess, non-equilibrium free volume, resulting from thermal rearrangement[6,10].

Hydrogen[25] and nitrogen[27] solubility in the TR samples at 35°C were calculated using the NELF model with one adjustable parameter, i.e., k_{12}. Sorption isotherms at all other temperatures

were predicted using, for each penetrant-polymer pair, the value of the binary parameter estimated at 35°C, as described above for HAB-6FDA. Fig. 4 shows the experimental data and the model fits for one sample, TR450-30min. Data for other TR samples are presented in the Supporting Information.

Methane solubility[27] can also be predicted with one fitting parameter, k_{12}. However, when considering the highly converted samples, i.e., TR400-1h and TR450-30min, a swelling coefficient was required to get a good representation of methane sorption data at temperatures below 10°C. At low temperatures, methane solubility in more highly converted samples increases considerably (it is comparable to CO_2 solubility at 20°C), so the occurrence of limited polymer dilation in the presence of methane at high pressures cannot be ruled out. However, the swelling coefficient values were very low (less than 0.008 MPa^{-1}, which is 8 times smaller than that needed in the case of CO_2 sorption in the same material at the same temperature), which is consistent with the limited matrix dilation expected for methane sorption in glassy polymers. If one assumes k_{sw} =0, the average deviation of model calculation from experimental sorption data is roughly -10% at pressures higher than 2MPa and temperatures lower than 10°C. As expected, no swelling coefficient is required to describe methane sorption data in TR400-1h and TR450-30 min at temperatures above 10°C.

The extent of volume dilation, $\Delta V/V_0$, induced by methane sorption in highly converted TR samples at -10°C and 2.5 MPa is estimated from the model to be less than 2%. This value compares reasonably well with that reported by Holck et al.[35], who measured the volume dilation induced by methane sorption at ambient temperature in 6FDA-TrMPD polyimide, PIM-

1, and polysulfone. Although the data reported by Holck[35] are for other polymers, they suggest that our estimate of dilation during methane sorption at low temperatures and high pressures in highly converted TR polymers is quantitatively reasonable. The swelling coefficients estimated for methane sorption at low temperatures in more highly converted samples are reported in Table S1 in the Supporting Information.

For carbon dioxide sorption[27], polymer dilation has to be taken into account at all temperatures considered. Thus, for each TR sample, the binary parameter k_{12} was optimized to the sorption isotherms at 35°C in the low pressure region, where dilation is negligible, and it was used to calculate the sorption isotherms at all other temperatures. The swelling coefficient, k_{sw}, was estimated by fitting the NELF model to the sorption data at high pressure, where significant matrix dilation was expected. The resulting set of fitting parameters is recorded in Table 4. As observed for CO_2 sorption in HAB-6FDA, the swelling coefficients estimated for the TR samples decrease with increasing temperature (cf., Fig. S4, Supporting Information).
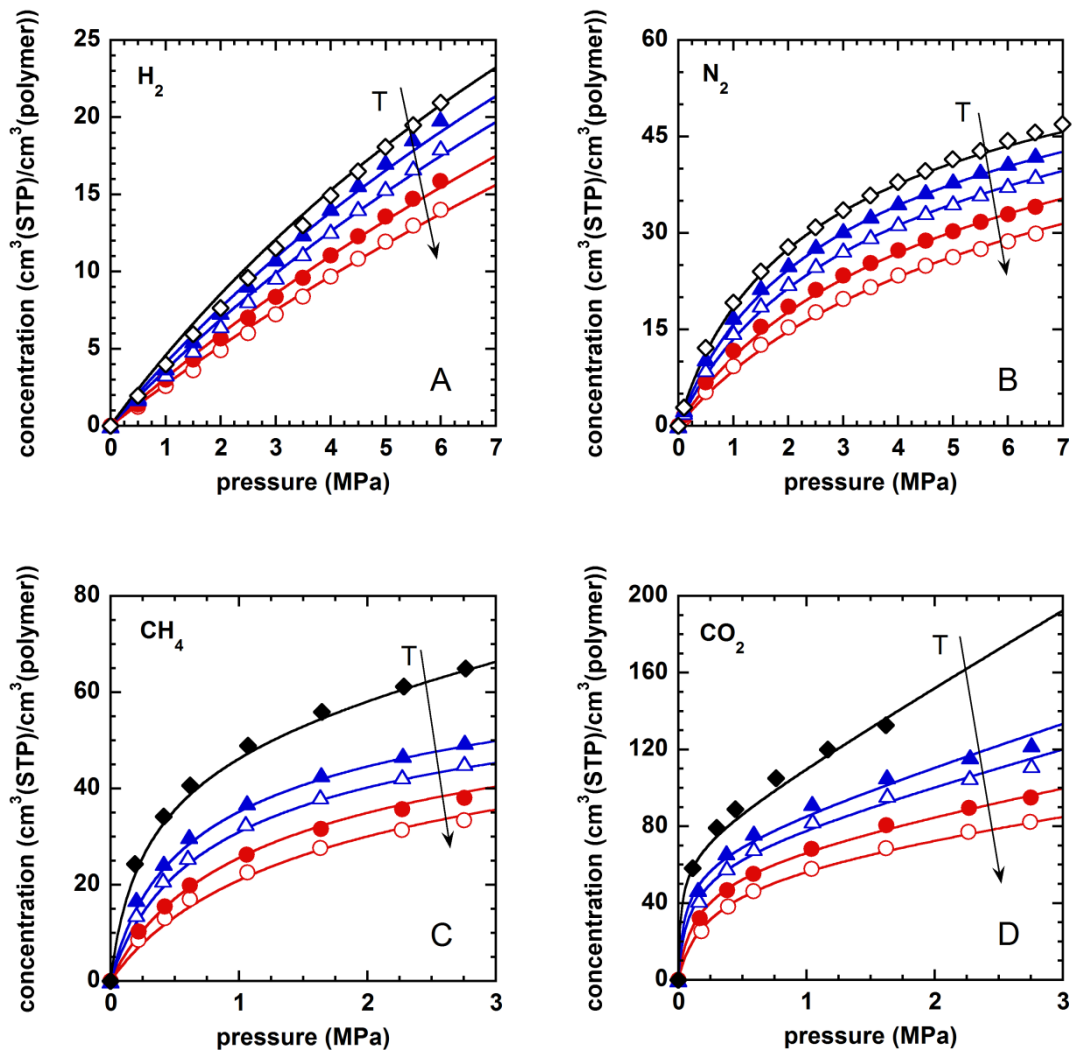
Figure 4. *Gas solubility in TR450-30min. A) H_2, B) N_2, C) CH_4, D) CO_2. Black filled diamonds: -10°C; black open diamonds: 0°C; blue filled triangles: 10°C; blue open triangles: 20°C; red filled circles: 35°C; red open circles: 50°C. Solid lines: NELF model calculations.*

The penetrant-polymer interaction becomes more and more favorable with decreasing values of k_{12}. For all penetrants considered, the binary interaction parameter, k_{12}, decreases slightly with increasing thermal conversion (cf., Table 4), indicating more favorable polymer-penetrant interactions in more highly converted samples. This trend reflects the structural changes undergone by the polymer upon thermal treatment and favors increases in gas sorption in more

highly converted samples. However, as presented in the next section, more favorable penetrant-polymer interactions only partially account for the observed increase in gas solubility in TR samples (cf., § 4.5).

For all the materials considered, H_2 has the most negative values of k_{12}. Large negative deviations from the Hildebrand rule were previously reported for hydrogen sorption in a series of glassy and rubbery polymers[17]. However, since H_2 is a sparingly soluble gas, the uncertainty in the sorption data (up to 8%) is greater than for other penetrants (less than 5%), so any molecular explanation of the large negative deviation of k_{12} from its standard value (i.e., zero) would be premature. CO_2 has slightly negative values of k_{12} in both the polyimide precursor and TR polymers, indicating that its interaction with polymers does not depart significantly from the Hildebrand's rule. Binary parameter for N_2 and CH_4 are positive and greater than those obtained in the case of H_2 and CO_2, which indicates that these gases have less favorable interaction with the polymers. However, the CH_4 binary parameter is somewhat lower than that of N_2, which is consistent with the hydrocarbon nature of methane.

The effect of uncertainty in polymer density on calculated sorption isotherms was estimated. If polymer density is allowed to change in its interval of confidence, the effect on lattice fluid parameters estimated from Eq. 2 is essentially negligible (< 2%), and the corresponding change in calculated gas solubility does not exceed 4%.

As mentioned previously, the lack of solubility in organic solvents indicates a possibly cross-linked structure of TR polymers[6,7,8]. The NELF model does not account for the effects of polymer cross-linking, which tend to reduce the solubility of low molecular weight compounds in

polymers[36]. However, the model provides a reasonable estimate of gas solubility in TR polymers, which is consistent with the relatively low sorbing nature of the gases considered in this study. Generally, for light gas sorption, polymer cross-link density has little effect on solubility[37]. A more significant effect of the polymer cross-linking on solubility would be expected if the penetrants were highly sorbing, condensable vapors[37].

4.4 Predicting volume dilation and solubility-selectivity. The model can be used to compare the dimensional stability of HAB-6FDA and its TR samples in the presence of swelling penetrants, such as carbon dioxide. The values of the swelling coefficient can be used to estimate the extent of matrix dilation induced by CO_2 sorption. The volume dilation can be estimated assuming isotropic swelling as a function of penetrant partial pressure (i.e., at any penetrant concentration in the polymer) as follows[12,22]:

$$\frac{V - V_0}{V_0} = \frac{k_{sw} p}{1 - k_{sw} p} \qquad \text{(Eq. 14)}$$

where V is the polymer volume when exposed to a penetrant at partial pressure p, and V_0 is the volume of the pure polymer before exposure to the swelling penetrant. In Fig. 5, the calculated volume dilation at 35°C is reported for the samples considered in this study as a function of CO_2 concentration in the polymer. Interestingly, at fixed CO_2 concentration, TR samples are predicted to exhibit less swelling (i.e., better dimensional stability) than that of the HAB-6FDA polyimide precursor. This result is consistent with the more rigid structure of TR polymers

relative to HAB-6FDA, as well as with the greater size and more favorable distribution of free volume elements in the TR analogs.
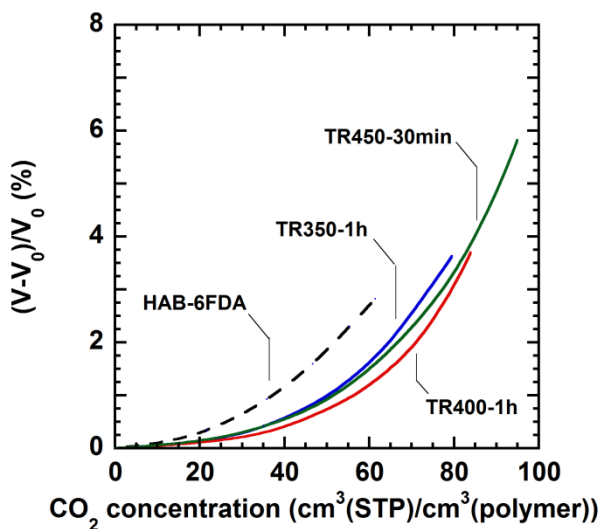
Figure 5. *Calculated CO_2 sorption induced dilation ($\Delta V/V_0\%$) at 35°C as a function of CO_2 concentration in the polymer. Volume dilation was calculated using Eq. 14.*

The ideal (i.e., pure gas) solubility-selectivity for different penetrant pairs can be estimated as the ratio of solubility coefficients at fixed pressure and temperature. In Fig. 6, the CO_2/CH_4 and CO_2/H_2 ideal solubility selectivities at 35°C and 2 MPa are presented as a function of CO_2 solubility. The model calculations agree reasonably well with the experimental values[6,25,26,27] for both HAB-6FDA polyimide and the TR samples.

26
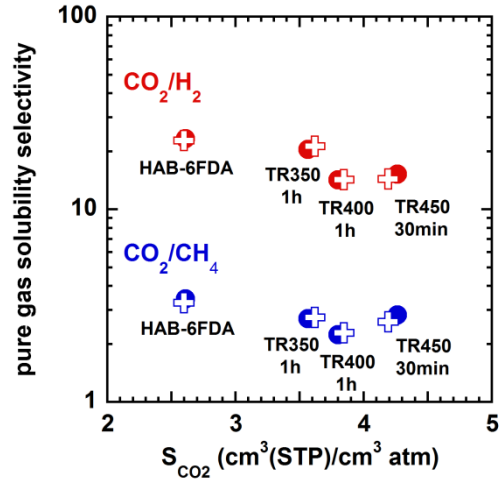
Figure 6. *Pure gas CO_2/CH_4 (blue circles) and CO_2/H_2 (red circles) solubility-selectivity for different polymers as a function of CO_2 sorption coefficient at 35 °C and 2 MPa. The crosses represent NELF model calculations.*

4.5 Thermodynamic analysis of gas sorption in TR polymers. The infinite dilution solubility coefficient contains an entropic contribution (ϕ_S) and an enthalpic contribution (ϕ_H) which cannot be evaluated experimentally. The NELF model provides an explicit expression for both contributions[12,28]. ϕ_S and ϕ_H depend on both penetrant and polymer properties, but, according to Eq. 13, only the enthalpic term, ϕ_H, depends explicitly on polymer-penetrant interactions.

In Fig. 7A-B, the enthalpic and entropic factors are presented as a function of the ratio T_c / T, where T_c is the penetrant critical temperature, and T is the experimental temperature. As reported by Galizia et al.[12] and by Sarti et al.[28], the enthalpic contribution is always positive and increases with increasing penetrant condensability (i.e., increasing penetrant critical temperature). The logarithm of S_{inf} is dominated by ϕ_H, since it always increases with increasing penetrant condensability[12,28]. The entropic contribution is always negative and

decreases with increasing critical temperature, since, when considering the sorption of bulky, more condensable penetrants, the probability of accommodating them inside the glassy matrix decreases with increasing molecular size[12,28]. Thus, the negative contribution of the entropic factor tends to reduce the solubility of more bulky penetrants in polymers.
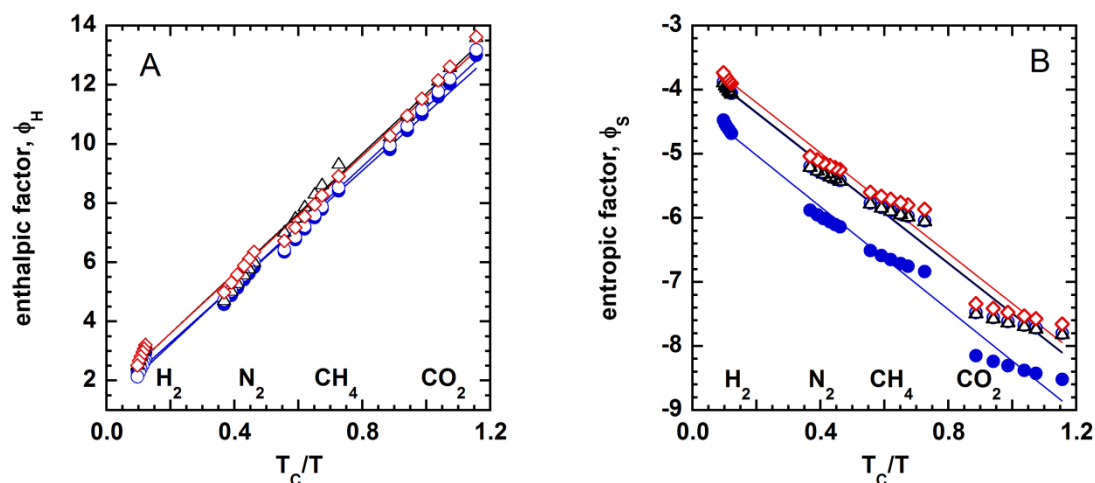
Figure 7. *Enthalpic (ϕ_H) and entropic (ϕ_S) contribution to $\ln(S_{inf})$, evaluated using Eqs. 12-13. Blue filled circles: HAB-6FDA; blue open circles: TR350-1h; black open triangles: TR400-1h; red open diamonds: TR450-30min. The solid lines are a guide for the eye.*

As shown in Fig. 7, conversion of HAB-6FDA polyimide to its corresponding TR polymers results in a barely detectable change in the enthalpic contribution to gas sorption. Conversely, the change in the entropic contribution is significant. In particular, ϕ_S is less negative in TR polymers than in the polyimide precursor. Thus, the increase in gas solubility observed with increasing extent of thermal conversion is due essentially to increases in the entropic factor. This result is consistent with the conclusions drawn by Smith et al.[6] Indeed, they infer that the greater sorption capacity of the TR samples relative to HAB-6FDA was due to the increase in non-equilibrium, excess fractional free volume upon thermal rearrangement. The increase in

free volume is accompanied by an increase in the probability of accommodating penetrant molecules in the polymer matrix, as confirmed by the substantial upward shift of ϕ_S in the TR samples. This relevant conclusion is also supported by the results of Dual Mode analysis of sorption data performed by Smith et al.[6]. While the Henry's law constant, k_D, and the Langmuir affinity parameter, b, did not exhibit any systematic trend with TR conversion, the Langmuir sorption capacity, C_H', systematically increased[6]. However, no other model permits separate calculation of the entropic and enthalpic contributions to gas solubility in polymers.

The theoretical analysis presented in this study confirms that the change in sorption behavior observed in TR polymers relative to that of their polyimide precursor is due to increases in excess, fractional free volume. The slight upward shift observed for the enthalpic contribution, ϕ_H, with increasing conversion also causes an increase in gas sorption capacity in TR polymers. This result is consistent with the general decreasing trend of k_{12}, for a given penetrant, with increasing conversion. As discussed above, polymer-penetrant interactions become more thermodynamically favorable in more highly converted samples, which promotes an increase in gas solubility in more highly converted TR polymers. However, the slight increase in the enthalpic contribution to solubility is overwhelmed by a more significant increase in the entropic counterpart, which is largely responsible for the observed increase in gas solubility in TR samples relative to HAB-6FDA polyimide.

Interestingly, these results are consistent with those reported by Smith et al.[25] when considering hydrogen sorption in TR polymers at different temperatures. They observed slight changes in the isosteric heats of sorption with increasing extent of thermal conversion, but significant

increases in the pre-exponential factor in the Van't Hoff equation, which correlates with entropy of sorption[25]. The refined thermodynamic analysis presented in this section provides a significant gain in fundamental understanding of gas sorption in TR polymers, and it rationalized previous experimental findings from a theoretical standpoint.

4.6 Enthalpy of sorption at infinite dilution. The sorption data in Figs. 2 and 4 show a significant dependence on temperature. The theoretical basis of temperature dependence of gas solubility in polymers is discussed in the Supporting Information. Regardless of the penetrant considered, gas sorption decreases with increasing temperature. This result is consistent with the typical exothermic sorption behavior exhibited by glassy polymers[17,38]. Remarkably, the NELF model captures the temperature dependence of gas solubility. In a recent publication, Galizia et al.[17] derived an explicit expression for the infinite dilution enthalpy of sorption:

$$\Delta H_{S,\text{inf}} = -R\left\{T + 2r_1^0 \frac{\rho_2^0}{\rho_2^*} T_1^* \left(1 - k_{12}\right)\sqrt{\frac{p_2^*}{p_1^*}}\right\} \qquad \text{(Eq. 15)}$$

where the symbols have the usual meaning. In Eq. 15, the polymer thermal dilation in neglected, i.e., polymer density is not allowed to change with temperature. As explained earlier, this assumption is reasonable, since the polymer density should change by no more than about 1% over the entire range of temperature considered. So, Eq. 15 allows an immediate estimate of sorption enthalpy at infinite dilution, since it does not contain any adjustable parameters.

As reported in Table 5, the experimentally determined $\Delta H_{S,\text{inf}}$ values are in reasonable agreement with NELF model predictions, with an average deviation of 44%. This deviation is

quantitatively similar to that reported by other authors when considering gas sorption in Teflon® AF at multiple temperatures[39]. In ref. 39, $\Delta H_{S,\text{inf}}$ was estimated by fitting the calculated infinite dilution sorption coefficients to the van't Hoff equation. Deviations from experimental values up to 48 % were observed. So, Eq. 15 represents an useful tool to calculate, with no additional adjustable parameter, enthalpies of sorption at infinite dilution. Moreover, using Eq. 15 is consistent with the approach based on the lattice fluid theory used in this study.

As expected, in the absence of specific penetrant-polymer interactions, the enthalpy of sorption becomes largely negative as penetrant condensability increases, i.e., $\Delta H_{S,\text{inf}}(H_2) > \Delta H_{S,\text{inf}}(N_2) > \Delta H_{S,\text{inf}}(CH_4) > \Delta H_{S,\text{inf}}(CO_2)$.

Table 5. Enthalpy of sorption at infinite dilution. Theoretical values were calculated using Eq.15. Experimental data are from literature[25,27].

	$\Delta H_{S,\text{inf}}$ (kJ/mol)							
	HAB-6FDA		*TR350-1h*		*TR400-1h*		*TR450-30min*	
	exp.	*calc.*	*exp.*	*calc.*	*exp.*	*calc.*	*exp.*	*calc.*
H_2	-6.20 ± 0.06	-8.58	-5.74 ± 0.13	-8.30	-5.33 ± 0.09	-8.40	-5.33 ± 0.09	-8.40
N_2	-15.9 ± 1.5	-16.9	-15.1 ± 0.73	-16.4	-13.0 ± 1.16	-16.4	-14.5 ± 0.54	-16.4
CH_4	-18.08 ± 3.0	-21.9	-14.9 ± 2.23	-21.3	-16.6 ± 1.80	-21.3	-18.7 ± 1.54	-21.3
CO_2	-29.12 ± 2.8	-30.4	-15.1 ± 2.0	-29.5	-21.6 ± 1.42	-29.5	-20.4 ± 1.30	-29.5

5. Conclusions

For the first time, a theoretical interpretation of gas sorption in glassy HAB-6FDA polyimide and in its thermally rearranged analogs is presented. A crucial point in this analysis is the estimation of the lattice fluid parameters for the polymers. The pVT data in the rubbery region

are not available for HAB-6FDA polyimide and are not experimentally accessible for TR polymers. Consequently, the lattice fluid parameters were estimated using a collection of gas sorption data in the limit of infinite dilution.

For non-swelling penetrants, such as hydrogen, nitrogen and methane, the NELF model provides a reasonably good description of the experimental sorption isotherms with one adjustable parameter. For swelling penetrants, such as carbon dioxide, a second adjustable parameter, the swelling coefficient, was used to describe the sorption isotherms in the high pressure region.

To investigate the molecular origin of the change in gas sorption behavior with increasing TR conversion, the enthalpic and the entropic contributions to the solubility coefficient were calculated. The increase in gas solubility with increasing TR conversion is essentially due to an increase in the entropic contribution, with the enthalpic counterpart being barely affected by thermal conversion. Thus, the increase in gas solubility observed in TR samples relative to HAB-6FDA polyimide is essentially due to the increase of excess, non-equilibrium fractional free volume.

Finally, the volume dilation induced by carbon dioxide sorption at 35°C in HAB-6FDA and its TR samples was calculated. As expected, TR samples exhibit less penetrant-induced swelling than the HAB-6FDA polyimide precursor.

The approach used in this study presents some advantages compared to other models for gas sorption in glassy polymers, since it provides a large amount of fundamental information with few adjustable parameters. In particular: *i)* it has good predictive capability; *ii)* the polymer

lattice fluid parameters correlate with TR conversion; *iii)* polymer swelling may be predicted; and *iv)* the experimental solubility coefficient can be decomposed into its enthalpic and entropic contributions, which provides valuable fundamental insights regarding gas sorption behavior of TR polymers.

Supporting Information. Additional tables and figures are provided in the Supplementary Information.

References

[1] Gleason, K.L.; Smith, Z.P.; Liu, Q.; Paul, D.R.; Freeman, B.D. Pure- and mixed-gas permeation of CO_2 and CH_4 in thermally rearranged polymers based on 3,3′-dihydroxy-4,4′-diamino-biphenyl (HAB) and 2,2′-bis-(3,4-dicarboxyphenyl) hexafluoropropane dianhydride (6FDA). *J. Membr. Sci.* **2015**, 475, 204-214

[2] Park, H.B.; Jung, C.H.; Lee, Y.M.; Hill, A.J.; Pas, S.J.; Mudie, S.T.; Van Wagner, E.; Freeman, B.D.; Cookson, D.J., Polymers with cavities tuned for fast selective transport of small molecules and ions. *Science* **2007**, 318, 254-258

[3] Robeson, L.M. The upper bound revisited. *J. Membr. Sci.* **2008**, 320, 390-400

[4] Woo, K.T.; Lee, J.; Dong, G.; Kim, J.S.; Do, Y.S.; Hung, W.S.; Lee, K.R.; Barbieri, G.; Drioli,E.; Lee, Y.M. Fabrication of thermally rearranged (TR) polybenzoxazole hollow fiber membranes with superior CO_2/N_2 separation performance. *J. Membr. Sci.* **2015**, 490, 129-138

[5] Cersosimo, M.; Brunetti, A.; Drioli, E.; Fiorino, F.; Dong, G.; Woo, K.T.; Lee, J.; Lee, Y.M.; Barbieri, G. Separation of CO_2 from humidified ternary gas mixtures using thermally rearranged polymeric membranes. *J. Membr. Sci.* **2015**, 492, 257-262

[6] Smith, Z.P.; Sanders, D.F.; Ribeiro, C.P.; Guo, R.; Freeman, B.D.; Paul, D.R.; McGrath, J.E.; Swinnea, S. Gas sorption and characterization of thermally rearranged polyimides based on 3,3'-dihydroxy-4,4'-diamino-biphenyl (HAB) and 2,2'-bis-(3,4-dicarboxyphenyl) hexafluoropropane dianhydride (6FDA). *J. Membr. Sci.* **2012**, 415-416, 558-567

[7] Sanders, D.F.; Smith, Z.P.; Ribeiro, C.P.; Guo, R.; McGrath, J.E.; Paul, D.R.; Freeman, B.D. Gas permeability, diffusivity, and free volume of thermally rearranged polymers based on 3,3'-dihydroxy-4,4'-diamino-biphenyl (HAB) and 2,2'-bis-(3,4-dicarboxyphenyl) hexafluoropropane dianhydride (6FDA). *J. Membr. Sci.* **2012**, 409-410, 232-241

[8] Smith, Z.P.; Czenkusch, K.; Wi, S.; Gleason, K.L.; Hernández, G.; Doherty, C.M.; Konstas, K.; Bastow, T.J.; Álvarez, C.; Hill, A.J.; Lozano, A.E.; Paul, D.R.; Freeman, B.D. Investigation of the chemical and morphological structure of thermally rearranged polymers. *Polymer* **2014**, 55, 6649–6657

[9] Liu, Q.; Galizia, M.; Gleason, K.L.; Scholes, C.A.; Paul, D.R.; Freeman, B.D. Influence of toluene on CO_2 and CH_4 gas transport properties in thermally rearranged (TR) polymers based

on 3,3'-dihydroxy-4,4'-diamino-biphenyl (HAB) and 2,2'-bis-(3,4-dicarboxyphenyl) hexafluoropropane dianhydride (6FDA). *J. Membr. Sci.* **2016**, 514, 282-293

[10] Jiang, Y.; Willmore, F.T.; Sanders, D.F.; Smith, Z.P.; Ribeiro, C.P.; Doherty, C.M.; Thornton, A.; Hill, A.J.; Freeman, B.D.; Sanchez, I.C. Cavity size, sorption and transport characteristics of thermally rearranged (TR) polymers. *Polymer* **2011**, 52, 2244-2254

[11] Robeson, L.M.; Dose, M.E.; Freeman, B.D.; Paul, D.R. Analysis of the Transport Properties of Thermally Rearranged (TR) Polymers and Polymers of Intrinsic Microporosity (PIM) Relative to Upper Bound Performance, submitted to J. Membr. Sci. **2016**

[12] Galizia, M.; De Angelis, M.G.; Sarti, G.C. Sorption of hydrocarbons and alcohols in addition-type poly(trimethyl silyl norbornene) and other high free volume glassy polymers. II: NELF model predictions. *J. Membr. Sci.* **2012**, 405-406, 201-211

[13] Sanchez, I.C.; Lacombe, R.H. Statistical thermodynamics of polymer solutions. *Macromolecules* **1978**, 11, 1145-1156.

[14] Doghieri, F.; Sarti, G.C. Non Equilibrium Lattice Fluid: a predictive model for the solubility in glassy polymers. *Macromolecules* **1996**, 29, 7885-7896

[15] Barrer, R.M.; Barrie, J.A.; Slater, J. Sorption and diffusion in ethyl cellulose. Part III. Comparison between ethyl cellulose and rubber. *J. Polym. Sci.* **1958**, 27, 177-197.

[16] Paul, D.R.; Koros, W.J. Effect of partially immobilizing sorption on permeability and the diffusion time lag. *J. Polym. Sci.: Polym. Phys. Ed.* **1976**, 14, 675-685

[17] Galizia, M.; Smith, Z.P.; Sarti, G.C.; Freeman, B.D.; Paul, D.R. Predictive calculation of hydrogen and helium solubility in glassy and rubbery polymers. *J. Membr. Sci.* **2015**, 475, 110-121

[18] Ferrari, M.C.; Galizia, M.; De Angelis, M.G.; Sarti, G.C. Gas and vapor transport in mixed matrix membranes based on amorphous Teflon AF1600 and AF2400 and fumed silica. *Ind. Eng. Chem. Res.* **2010**, 49, 11920-11935.

[19] Galizia, M.; De Angelis, M.G.; Messori, M.; Sarti, G.C. Mass transport in hybrid PTMSP/Silica membranes, *Ind. Eng. Chem. Res.* **2014**, 53, 9243-9255

[20] Ferrari, M.C.; Galizia, M.; De Angelis, M.G.; Sarti, G.C. In *Membrane Gas Separation*; B.D. Freeman, Y. Yampolskii, Eds.; Wiley: New York, 2010, p. 125-142.

[21] Hildebrand, J.H.; Prausnitz, J.M.; Scott, R.L. *Regular and related solutions: the solubility of gases, liquids and solids*, Van Nostrand Reinhold, New York, 1970.

[22] Galizia, M.; De Angelis, M.G.; Finkelshtein, E.; Yampolskii, Y.; Sarti, G.C. Sorption and transport of hydrocarbons and alcohols in addition-type poly(trimethyl silyl norbornene). I: Experimental data. *J. Membr. Sci.* **2011**, 385-386, 141-153

[23] Giacinti Baschetti, M.; Doghieri, F.; Sarti, G.C. Solubility in glassy polymers: correlations through the Non-equilibrium Lattice Fluid Model. *Ind. Eng. Chem. Res.* **2001**, 40, 3027-3037

[24] Minelli, M.; Cocchi, G.; Ansaloni, L.; Giacinti Baschetti, M.; De Angelis, M.G.; Doghieri, F. Vapor and liquid sorption in Matrimid polyimide: experimental characterization and modeling, *Ind. Eng. Chem. Res.* **2013**, 52, 8936-8945

[25] Smith, Z.P.; Tiwari, R.R.; Murphy, T.M.; Sanders, D.F.; Gleason, K.L.; Paul, D.R.; Freeman, B.D. Hydrogen sorption in polymers for membrane applications. *Polymer* **2013**, 54, 3026-3037.

[26] Smith, Z.P.; Tiwari, R.R.; Dose, M.E.; Gleason, K.L.; Murphy, T.M.; Sanders, D.F.; Gunawan, G.; Robeson, L.M.; Paul, D.R.; Freeman, B.D. The influence of diffusivity and sorption on helium and hydrogen separations in hydrocarbon, silicon, and fluorocarbon-based polymers. *Macromolecules* **2014**, 47, 3170-3184.

[27] Stevens, K.A.; Smith, Z.P.; Gleason, K.L.; Galizia, M.; Paul, D.R.; Freeman, B.D. Influence of temperature on gas solubility in thermally rearranged polymers, to be submitted to the *Journal of Membrane Science*, **2016**.

[28] De Angelis, M.G.; Sarti, G.C.; Doghieri, F. NELF model prediction of the infinite dilution gas solubility in glassy polymers. *J. Membr. Sci.* **2007**, 289, 106-122.

[29] Scherillo, G.; Sanguigno, L.; Galizia, M.; Lavorgna, M.; Musto, P.; Mensitieri, G. Non-equilibrium compressible lattice theories accounting for hydrogen bonding interactions: Modelling water sorption thermodynamics in fluorinated polyimides. *Fluid Ph. Eq.* **2012**, 334, 166-188.

[30] Matrimid 5218 Product Data, www.huntsman.com (09/20/2015).

[31] Zoller, P.; Walsh, D. *Standard pressure-volume-temperature data for polymers*, Technomic, Lancaster, 1995.

[32] Bevington, P.R.; Robinson, D.K. *Data reduction and error analysis for the physical sciences*, 3rd Ed., McGraw-Hill, Boston, 2003.

[33] Bondar, V.I.; Kamiya, Y.; Yampolskii, Y. On pressure dependence of the parameters of the Dual-Mode Sorption Model. *J. Polym. Sci. B: Polym. Phys.* **1996**, 34, 369-378.

[34] Fleming, G.K.; Koros, W.J.; Dilation of polymers by sorption of carbon dioxide at elevated pressures. 1. Silicone rubber and unconditioned polycarbonate. *Macromolecules* **1986**, 19, 2285-2291.

[35] Hölck, O.; Böhning, M.; Heuchel, M.; Siegert, M.R.; Hofmann, D. Gas sorption isotherms in swelling glassy polymers—Detailed atomistic simulations. *J. Membr. Sci.* **2013**, 428, 523–532.

[36] Flory, P.J.; Rehner, J. Statistical mechanics of cross-linked polymer networks II. Swelling. *J. Chem. Phys.* **1943**, 11, 521-526.

[37] Ribeiro, C.P.; Freeman, B.D. Carbon dioxide/ethane mixed gas sorption and dilation in a crosslinked poly(ethylene oxide) copolymer. *Polymer* **2010**, 51, 1156-1168.

[38] Koros, W.J.; Paul, D.R.; Huvard, G.S. Energetics of gas sorption in glassy polymers. *Polymer* **1979**, 20, 956-960.

[39] De Angelis, M.G.; Merkel, T.C.; Bondar, V.I.; Freeman, B.D.; Doghieri, F.; Sarti, G.C. Gas sorption and dilation in poly(2,2-bistrifluoromethyl-4,5-difluoro-1,3-dioxole-co-tetrafluoroethylene): comparison of experimental data with predictions of the Non-equilibrium Lattice Fluid Model. *Macromolecules* **2002**, 35, 1276–1288.